CHAPTER
5 THREE PHASE OPERATION OF BLDC MOTOR USING MODIFIED SINUSOIDAL PULSE WIDTH MODULATION TECHNIQUE

The Brushless DC motor when operated with 2-ΦO and 2-3ΦO as discussed in the previous chapters with quasi square wave current in phase with trapezoid back emf leads to finite torque ripple in the commutation region with only two phases conducting at any time. To overcome this, the BLDC motor phases can be supplied with sinusoidal currents which reduce the voltage required to deal with the phase inductance instead of quasi square currents as the change in currents is smoother because of its shape. This chapter provides analysis and implementation of a simple closed control technique using the Modified Sinusoidal Pulse Width Modulation Technique (MSPWM) to improve the performance of BLDC motor with 3-ΦO with reduced commutation torque ripple and improved DC bus utilization. To prove the effectiveness of the technique, it is compared with the conventional six-step operation of the BLDC motor as discussed in chapter 2.

5.1 Introduction

To overcome the disadvantages and boost the adaptability of BLDC motor drive many control techniques and approaches have been provided. Halfway during the ninties, Kirnnich, Heinrick, and Bowes developed the first modulation technique to bring the output voltage and current of the converter nearer to the sine wave. The repercussions of advanced commutation angle on the current harmonics and phase current is studied by [78]. The harmonics in the torque along with ripple changes with the commutation angle which can be reduced by choosing appropriate control strategies and improved motor design. A pseudo-dq technique is proposed by [79] for non-sinusoidal back emf BLDC motors to compare the efficiency of the drive as compared to the conventional dq theory for minimizing torque ripple. The author [80] focused on the modulation index(MI) which is said to be determining factor for the PWM techniques. The maximum MI obtained using the sinusoidal PWM (SPWM) technique is 0.785 when a sinusoid reference signal is compared with a ramp signal. A flat-topped reference signal whose peak value is less than fundamental can be generated by a adding third harmonic to obtain a higher value of MI.

The dq axis model of permanent magnet machine by using the concept of extended Park transformation by incorporating arbitrary flux patterns for implementing vector control of non -sinusoid back emf machine to scale back the variation in torque and enhance the pursuance of the drive is suggested by [81]. A study on trapezoidal, sinusoidal and field-oriented commutation strategies for the BLDC motor and PMSM and optimum performance of the drive can be obtained by selecting the precise commutation strategy for a particular motor type is incorporated by [82]. The BLDC motor when operated with modified sinusoidal PWM technique has 6N harmonic torque instead of pulsating torque and the torque ripple is reduced up to 50% than conventional six-step control [83]. The closed-loop operation is not discussed which shows poor dynamic response of the drive which limits its application. The BLDC motor operating with any type of back emf whether sinusoidal or trapezoidal, the stator copper loss is increased by 10.2% when operated with quasi square wave currents as compared to the vectorial waveform currents as the RMS value of square wave current is greater than the vectorial currents[84]. The author [85] pointed out the sinusoidal currents with trapezoidal back emf for BLDC motor are most suitable for high-speed operation of the drive. Two different FW-SVCs algorithms in two different synchronous reference frames and enlightens the pros and cons of both methods. The FW-SVC-φτ techniques discussed by them also approve that sinusoidal currents with non -sinusoidal back emf provide improved drive performance for BDC motor with increased torque ripple at low speed is discussed by [86]. The work done in[87] shows that for all ranges of speed, the performance of the drive with sinusoidal supply currents outlays the drive performance using quasi-square wave currents. The space vector modulation technique(SVM) is used to produce sinusoidal current to prove the performance improvement of the BLDC motor drive with respect to the conventional operation with square wave current. The paper provides the comparison of sinusoidal currents and square wave currents at different speeds. A current optimization control is suggested by [88] over the square wave current control technique in a stationary reference frame to mitigate commutation torque ripple. An improved direct torque control(DTC) technique using two-phase and three-phase conduction to minimize the commutation torque ripple is proposed by [89]. A simple overlap angle strategy for commutation torque ripple minimization using two-phase and three-phase conduction over the six-step DTC and twelve-step DTC techniques is incorporated by [90].

Since conventionally BLDC motor is excited with quasi square wave currents, it leads to produce commutation torque ripple due to finite inductance of winding during commutation interval. The commutation torque ripple produces adverse effects on motor performance like jerks, unwanted noise, vibrations, etc. In this work, it is attempted to reduce commutation torque ripple using sinusoidal excitation at the same time improve the DC link utilization. Since the proposed MSPWM technique leads motor control in three-phase conduction mode, it naturally offers three-phase conduction during commutation interval which helps to reduce commutation torque ripple in BLDC motor.

The proposed technique aims to develop closed-loop speed control of BLDC motor with reduced torque ripple by providing sinusoidal stator currents in synchronism with the trapezoidal back emf. To improve the dynamic response, the closed-loop operation is proposed in this work. Simultaneously, the effect of sinusoidal excitation on torque ripple is also analyzed. Moreover, the proposed technique uses only one PI controller to produce sinusoidal currents which reduce control complexity. This chapter discusses and verifies the closed-loop operation of the drive-by performing simulation using MATLAB®/SIMULINK at different speeds and load with the MSPWM technique and compare the results with the conventional six-step motor control. An encoder is used to obtain instantaneous rotor position for the MSPWM technique and hall sensors are used to detect initial rotor position. The simulation results obtained using both techniques are compared to prove the effectiveness of the proposed method. To validate the proposed method it is tested on a prototype motor with a shaft encoder at high and low speed.

This chapter outlines the discussion of the overall system configuration of MSPWM technique with detailed analysis which includes: basic principle of FOC technique, modeling of MSPWM for BLDC motor drive, delta angle calculation, speed control of the motor, commutation logic circuit for 3-Φ Inverter, the simulation results and its discussion, the experimental verification of the MSPWM technique implemented on the BLDC motor drive followed by conclusions.

5.2 Principle of FOC

The FOC technique is used to de-couple the torque and flux components. For DC motors, the MMF produced by the armature winding and field winding is orthogonal making the flux and torque to be independently controlled. As the motor flux is merely generated by field excitation, the torque control can be achieved by armature current by keeping the flux constant.

For AC machines, the flux and torque components are not orthogonal to each other. With permanent magnet BLDC motors, the flux being constant with the rotor being of a permanent magnet, the torque can be controlled by controlling the stator currents. Using the FOC technique, the de-coupling of the torque and flux is achieved by transforming three-phase stator currents from the stationary reference frame to the torque and flux producing quantities in the rotating reference frame widely known as the d-q reference frame. The performance of the AC machines can be improved by using the FOC technique. With the three-phase currents i_a, i_b, and i_c transformed into the phase quantities i_d (direct axis current) and i_q (quadrature axis current). The i_d current resembling the stator flux component should be aligned with the rotor axis(d-axis) and i_q current representing the stator torque component(q-axis) should be maintained at 90° with the rotor axis. With i_d in the same direction as the rotor flux results in the increase in the net air gap flux with the addition of stator flux to the rotor flux. For flux weakening operation, with negative i_d, the stator flux opposes the rotor flux with the net reduction in the air gap flux producing lesser torque ripple.

Using the FOC technique, Maximum Torque Per Ampere (MTPA) ratio can be achieved by controlling the i_d and i_q currents independently with the reduced current requirement providing maximum motor efficiency. With the different rotor construction, there is a difference in the reluctance in the air gap flux path. This affects the saliency of the machine. As shown in Fig. 2.1, the surface-mounted rotor construction provides increased air gap length increasing the air gap reluctance resulting in reduced magnetizing inductance. With interior permanent magnet construction, the air gap is reduced resulting in higher magnetizing inductance.

For a non-salient pole machine with the surface-mounted rotor construction with $L_d= L_q$, the reluctance torque is zero. The direct axis current id is considered to be zero and does not affect the production of torque. Only the q axis current is considered to achieve the MTPA condition. For a salient pole machine, the higher magnetizing inductance, the parameters $L_d \neq L_q$ makes the motor control complex. With the FOC faster response of the torque and flux is achieved. The FOC technique can be implemented by controlling the magnitude of the stator voltage or current for the BLDC motor to achieve torque control for improved motor performance.

5.3 System description with modified sinusoidal pulse width technique for 3-ΦO

The block diagram is proclaimed in Fig.5.1 for the analysis of drive performance using the MSPWM technique for the BLDC motor. In this technique, a BLDC motor with trapezoidal back emf is operated with sinusoidal stator currents to generate optimal torque per ampere current. The three phases of the motor stator winding are supplied through an electronic commutator.

The recognition of rotor poles is mandatory for a sensored drive to decide the commutation logic for the three-phase stator winding by relevant switching of the inverter switches. Three-position sensors with an encoder are provided to decode the exact rotor position to generate six commutation states in one electrical cycle. The rotor position and speed are obtained using an encoder. To realize the six commutation instances, three hall sensors are incorporated in the stator such that when they are covered by magnetic “N” pole they conduct. Maximum two hall sensors are covered by “N” Pole and at least one hall sensor remains under the influence of “N” pole at any time as discussed [91].

Initially, the motor is started using the status of HES. The stator flux is changed following the rotor position. Maximum torque per ampere is produced when the rotor flux follows the stator flux by an angle of 90˚. The optimal delta angle (δ) is calculated by transforming the three-phase stator currents into a rotating dq axis reference frame from abc reference frame using Park's transformation. The motor speed is calculated from the rotor position and compared with the quoted speed. The difference between the two speeds is fixed by a PI controller. The gain of the controller controls the magnitude of the three-phase voltages by the virtue of the modulation index. Three-phase sinusoidal voltages are generated in the voltage generation block using the delta angle, modulation index, and electrical rotor position. Three saddle shape modulating waves are generated which are matched with the triangular carrier wave to engender the gate pulses for the six inverter switches by the PWM modulator block. As variation in speed is in straight proportion to the applied voltage, motor control is inhibited by varying the duty cycle of the gate pulses.

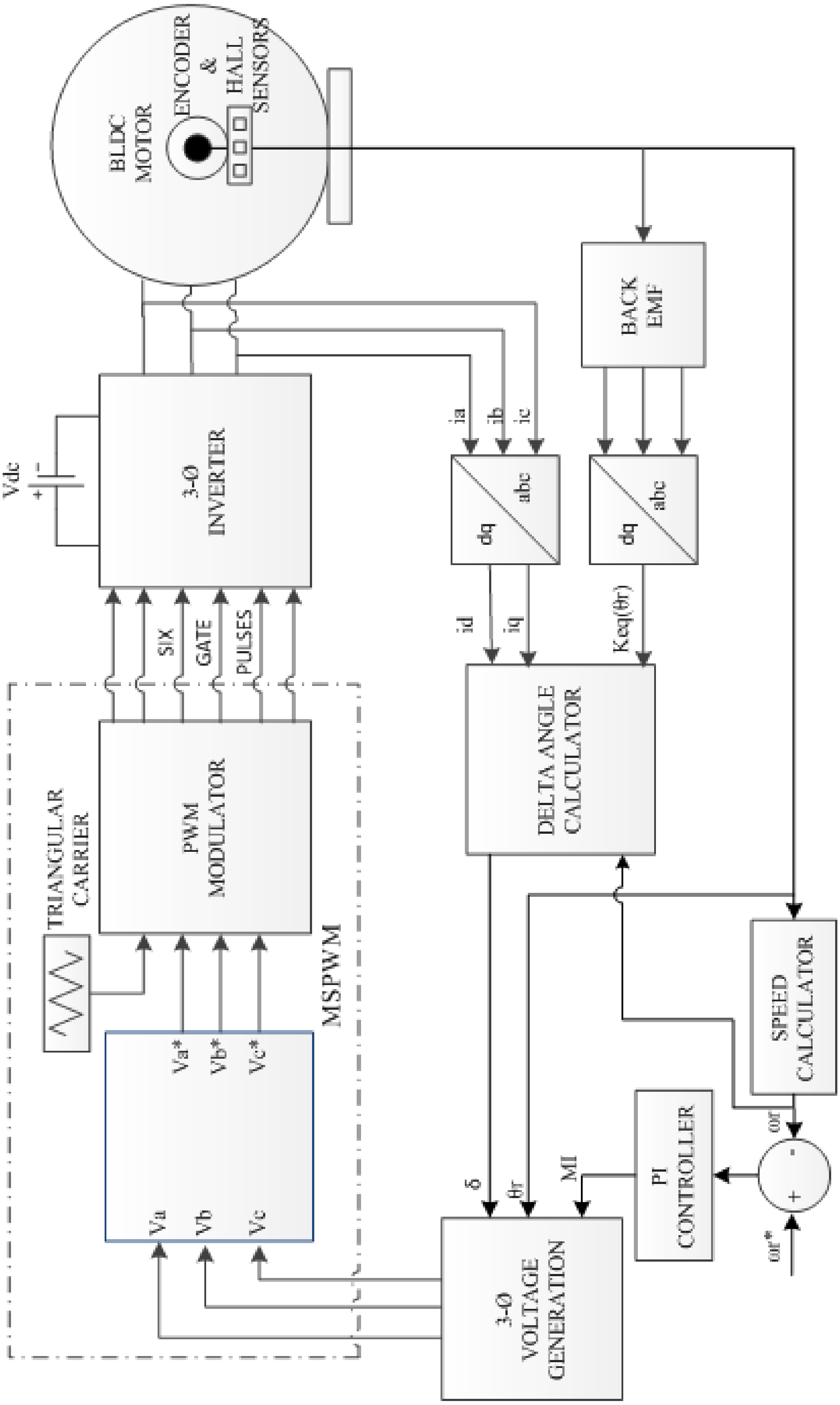

Fig. 5.1 Schematic block diagram of the overall system with MSPWM technique

5.3.1 Mathematical modeling of modified sinusoidal pulse width modulation technique for BLDC drive

Intending to obtain sine currents, dq transformation of all the variables defined in the abc reference frame is carried out using Park transformation. The dynamic equations of the BLDC motor described in eq. (2.1) to eq. (2.6) are transformed in the dq reference frame using eq. (5.1) to eq. (5.6).

$$(f_{qdos})^T = [f_{qs} f_{ds} f_{os}] \tag{5.1}$$

$$(f_{abcs})^T = [f_{as} f_{bs} f_{cs}] \tag{5.2}$$

$$(f_{qdos})^T = \mathrm{K}_s (f_{abcs})^T \tag{5.3}$$

$$\mathrm{K}_s = \frac{2}{3}\begin{bmatrix} \cos\theta_r & \cos(\theta_r - 2\pi/3) & \cos(\theta_r + 2\pi/3) \\ \sin\theta_r & \sin(\theta_r - 2\pi/3) & \sin(\theta_r + 2\pi/3) \\ 1/2 & 1/2 & 1/2 \end{bmatrix} \tag{5.4}$$

$$\begin{bmatrix} f_{ds} \\ f_{qs} \\ f_{os} \end{bmatrix} = \frac{2}{3}\begin{bmatrix} \cos\theta_r & \cos(\theta_r - 2\pi/3) & \cos(\theta_r + 2\pi/3) \\ \sin\theta_r & \sin(\theta_r - 2\pi/3) & \sin(\theta_r + 2\pi/3) \\ 1/2 & 1/2 & 1/2 \end{bmatrix}\begin{bmatrix} f_{as} \\ f_{bs} \\ f_{cs} \end{bmatrix} \tag{5.5}$$

$$(\psi_{dqos})^T = [\psi_{ds} - \psi_{qs} 0] \tag{5.6}$$

In the above equation parameter f can be a voltage, current, or flux linkage. The zero sequence components are neglected for a balanced three-phase system. The stator currents in abc frame are transformed in a rotating reference frame fixed on the rotor using Park transformation to get rid of the time-varying inductances. The dynamic equations after applying the dq transformation can be expressed as below. As the rotor rotates, the angle (θ_r) between the rotor and stator axis changes as discussed by [92][93] is shown in Fig. 5.2. A shaft encoder is used to obtain the angle (θ_r) between the stator magnetic field and rotor magnetic field.

To achieve optimum torque, it is necessary to control the q axis current (i_q) and d axis current (i_d). The current requirement to produce maximum torque is lessened by the maximal torque per ampere (MTPA) technique which minimizes the stator copper losses and maximizes the efficiency of the motor as suggested in [83][84].

$$V_{ds}^{r} = r_s i_{ds}^{r} + p\psi_{ds}^{r} - \omega_r \psi_{qs}^{r} + \omega_r \mathrm{K}_{ed}^{r}(\theta_r) \quad 5.7$$

$$V_{qs}^{r} = r_s i_{qs}^{r} + p\psi_{qs}^{r} + \omega_r \psi_{ds}^{r} + \omega_r \mathrm{K}_{eq}^{r}(\theta_r) \quad 5.8$$

$$\psi_{ds}^{r} = L_d i_{ds}^{r} \quad 5.9$$

$$\psi_{qs}^{r} = L_q i_{qs}^{r} \quad 5.10$$

Considering the BLDC motor with non -salient poles(Lq = Ld = Ls) helps to simplify above expressions

$$L_q = L_d = L_s \quad 5.11$$

$$\begin{bmatrix} V_{ds}^{r} \\ V_{qs}^{r} \end{bmatrix} = \begin{bmatrix} r_s + p\psi_{ds}^{r} & -\omega_r L_s \\ \omega_r L_s & r_s + p\psi_{qs}^{r} \end{bmatrix} \begin{bmatrix} i_{ds}^{r} \\ i_{qs}^{r} \end{bmatrix} + \omega_r \begin{bmatrix} \mathrm{K}_{ed}^{r}(\theta_r) \\ \mathrm{K}_{eq}^{r}(\theta_r) \end{bmatrix} \quad 5.12$$

$$\mathrm{T}_{em} = \frac{3}{2}\frac{p}{2}(\psi_{ds}^{r} i_{ds}^{r} - \psi_{qs}^{r} i_{qs}^{r}) \quad 5.13$$

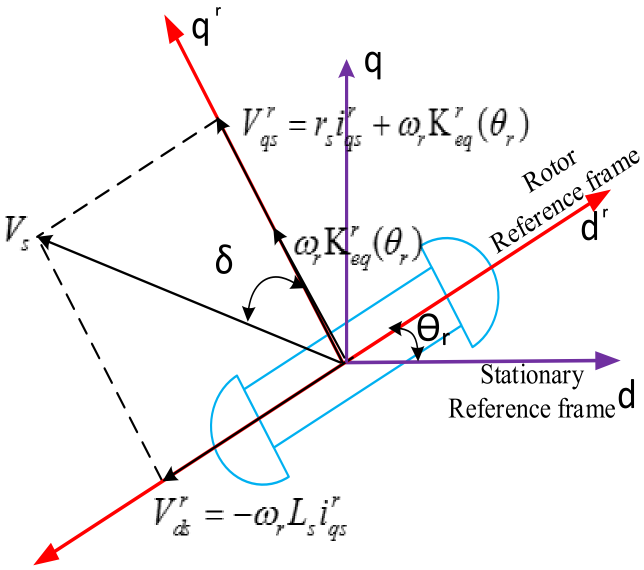

Fig. 5.2 Voltage vector representation

Table 5.1 Hall sensor output and inverter switching states

H_a	H_b	H_c	S1	S2	S3	S4	S5	S6
1	0	1	1	-	-	1	-	-
1	0	0	1	-	-	-	-	1
1	1	0	-	-	1	-	-	1
0	1	0	-	1	1	-	-	-
0	1	1	-	1	-	-	1	-
0	0	1	-	-	-	1	1	-

5.3.2 Delta angle calculation

For non-salient machines, optimal torque is obtained from the q-axis current and hence the d axis current is considered to be zero in eq. (5.7) to eq. (5.13) for a surface-mounted BLDC motor with a salient pole rotor as the reluctance torque is not developed. At the same time when the motor is operated with MTPA using the MSPWM technique, sinusoidal stator currents are produced which reduces the stator copper losses is quoted in [83][84]. The voltage and electromagnetic torque equations are modified as shown below equations.

$$V_{ds}^{r} = -\omega_r L_s i_{qs}^{r} \qquad 5.14$$

$$V_{qs}^{r} = r_s i_{qs}^{r} + \omega_r \mathrm{K}_{eq}^{r}(\theta_r) \qquad 5.15$$

$$\mathrm{T}_m = \frac{3}{2}\frac{p}{2}(\psi_{qs}^{r} i_{qs}^{r}) \qquad 5.16$$

From eq.(5.16) it can be observed that the motor electromagnetic torque is directly controlled by the quadrature axis current [94]. For accurate control of the BLDC motor drive, the stator currents should be in synchronism with the back emf. Since the back emf is a function of theta displaced with reference to stator magnetic field, it is necessary to determine the angle between stator field and rotor field**.** This angle is known as delta angle or displacement angle. To implement the MSPWM technique, an optimal delta angle (δ) is obtained using eq.(5.17).

$$\delta = \tan^{-1}\left(\frac{\omega_r L_s i_{qs}^{r}}{r_s i_{qs}^{r} + \omega_r \mathrm{K}_{eq}^{r}(\theta_r)}\right) \qquad 5.17$$

5.3.3 Speed control of BLDC motor drive

The control of speed in the BLDC motor drive is realized by controlling the duty ratio of the six gate pulses fed to the 3-Φ VSI which in turn regulates the DC bus voltage. For this, a PI controller is used as it is a resilient and most trusted controller.

$$MI = K_p e(t) + K_i \int e(t) d(t) \qquad 5.18$$

where,

MI = Modulation Index

e(t) = error signal of speed

K_p = proportionality gain

K_i = integral gain

The actual motor speed obtained from an encoder is mapped with the set speed. The difference between the two is processed by the PI controller. The controlled output signal thus obtained which is Modulation Index (MI) here, is used to generate three-phase sinusoidal voltages. The three reference modulating signals are generated to improve the modulation index as compared to the sinusoidal PWM technique. These modulating signals are processed in a PWM modulator block which compares them with high-frequency carrier waves to produced six gate pulses. The maximum output is obtained by changing the duty ratio to unity. The implemented speed control method is simple and does not require hysteresis controllers, sector selector, or torque estimator which reduces the complexity of the overall system. The added advantage of this method is reduced torque ripple as compared to sinusoidal pulse width modulation technique as well as six-step control.

5.3.4 Commutation logic circuit

In BLDC motor drive, the 3-Φ VSI acts like an electronic commutator that supplies three-phase current inaccurate dimensions with the rotor position to produce required torque. For this, three-phase terminal voltages are generated based on the modulation index, inverter pole voltage, and the modulating signal as given in eq. (5.19).

$$V_a = \frac{V_{dc}}{2} * MI * Sin(\theta_r + \delta + \frac{\pi}{2})$$

$$V_b = \frac{V_{dc}}{2} * MI * Sin(\theta_r - \frac{2\pi}{3} + \delta + \frac{\pi}{2}) \qquad 5.19$$

$$V_c = \frac{V_{dc}}{2} * MI * Sin(\theta_r + \frac{2\pi}{3} + \delta + \frac{\pi}{2})$$

The rotor angle δ is estimated using machine parameters, speed measured using an encoder, dq axis current, and back emf constant ($K^r_{eq}(\theta_r)$); where θ_r is calculated using eq. (2.6). The initial rotor position is obtained using hall sensors. In the sinusoidal pulse width modulation technique, three sine reference waves are compared with the triangular waves to generate gate pulses. Modulation index (MI) is the relation between the peak magnitudes of the modulating waveform and the carrier waveform. It relates the voltage of the DC link and the magnitude of pole voltage (fundamental component) output by the inverter. The value of MI determines the pulse width of the average pole voltage. It varies between 0<MI<1.

In modified SPWM three saddle shape modulating signals are generated using eq. (5.20) which is compared with the triangular carrier wave which increases the inverter output voltage by 15% . This improves the DC bus voltage utilization. The min (Va, Vb, Vc) indicates instantaneous minimum values of the three-phase voltages.

$$\begin{aligned} V_a{}^* &= V_a - \min(V_a, V_b, V_c) \\ V_b{}^* &= V_b - \min(V_a, V_b, V_c) \\ V_c{}^* &= V_c - \min(V_a, V_b, V_c) \end{aligned} \qquad 5.20$$

5.4 Simulation result and discussion

. The realization of the MSPWM technique is carried in MATLAB®/SIMULINK environment to obtain improved BLDC motor performance as compared to conventional six-step operation. The basic concept 2-ΦO of BLDC motor operation with SSC is discussed in chapter 2. The analysis for the same with the theoretical concept of the commutation sequences is provided which forms the basis of the simulation. The motor is tested under different speed and load conditions with the proposed technique and conventional SSC. The results of the proposed technique are compared with conventional SSC at different speeds and loading conditions.

Comparison between the six-step control technique and the MSPWM technique is shown at a speed of 2500 rpm with 5 Nm load in Fig.5.3a) and Fig. 5.3(b) respectively for the following parameters (i) rotor position (θ) (ii) hall output (Ha) (iii) gate pulses to switch S1 (iv) motor back emf (ea) (v) stator current (Ia) (vi) speed (N) (vii) motor torque (Tm). The conventional technique produces quasi square wave stator current in phase with the trapezoid back emf producing large torque ripple due to the mismatch in the slope of rising current and outgoing current with two phases conducting at any time. With the MSPWM technique, a sinusoidal current is produced in phase with the motor trapezoidal back. It can also be observed that the duty ratio is increased resulting in improved DC bus utilization using the proposed technique.

The ripple in the torque with the MSPWM technique is comparatively less at the same speed and applied load which leads to improved drive operation. Comparing Fig. 5.3(b) and 5.3(c) it can be noticed that at the same speed with an applied load torque reduced to half, the current is halved. The fine-tuning of the PI controller leads to the operation of the motor at its set speed under varied load conditions.

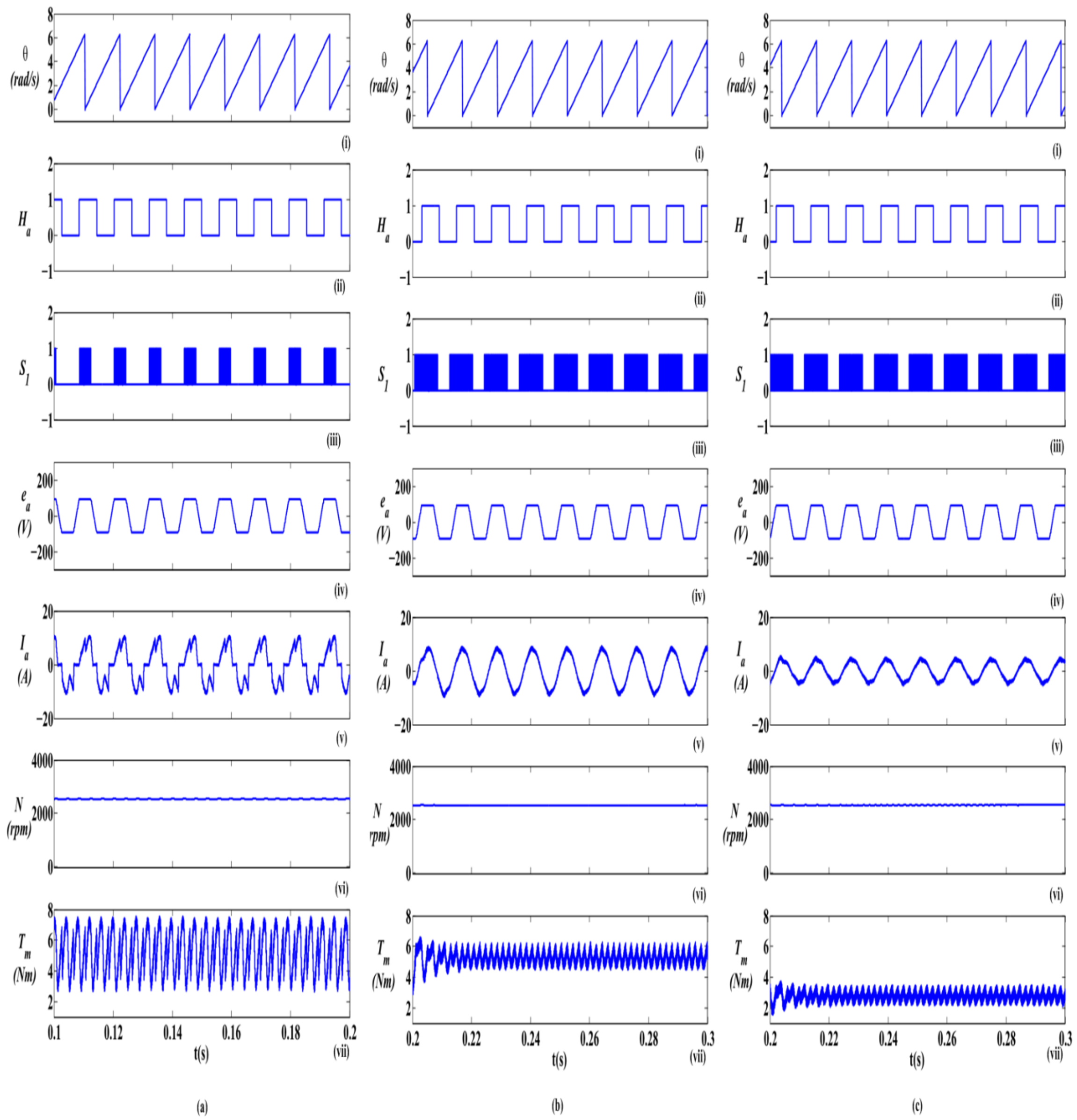

Fig. 5.3 Performance comparison of BLDC motor with (a) Conventional SSC technique at a speed of 2500 rpm with an applied load of 5 Nm (b) MSPWM technique at a speed of 2500 rpm with applied load of 5 Nm (c) MSPWM technique at a speed of 2500 rpm with applied load of 2.5 Nm

A similar comparison of conventional BLDC motor operation with the six-step control and the proposed MSPWM technique at a speed of 3000 rpm with an applied load of 2.5Nm can be observed in Fig.5.4(a) and (b). The figure clearly demonstrate the increase in DC bus utilization with sinusoidal currents.

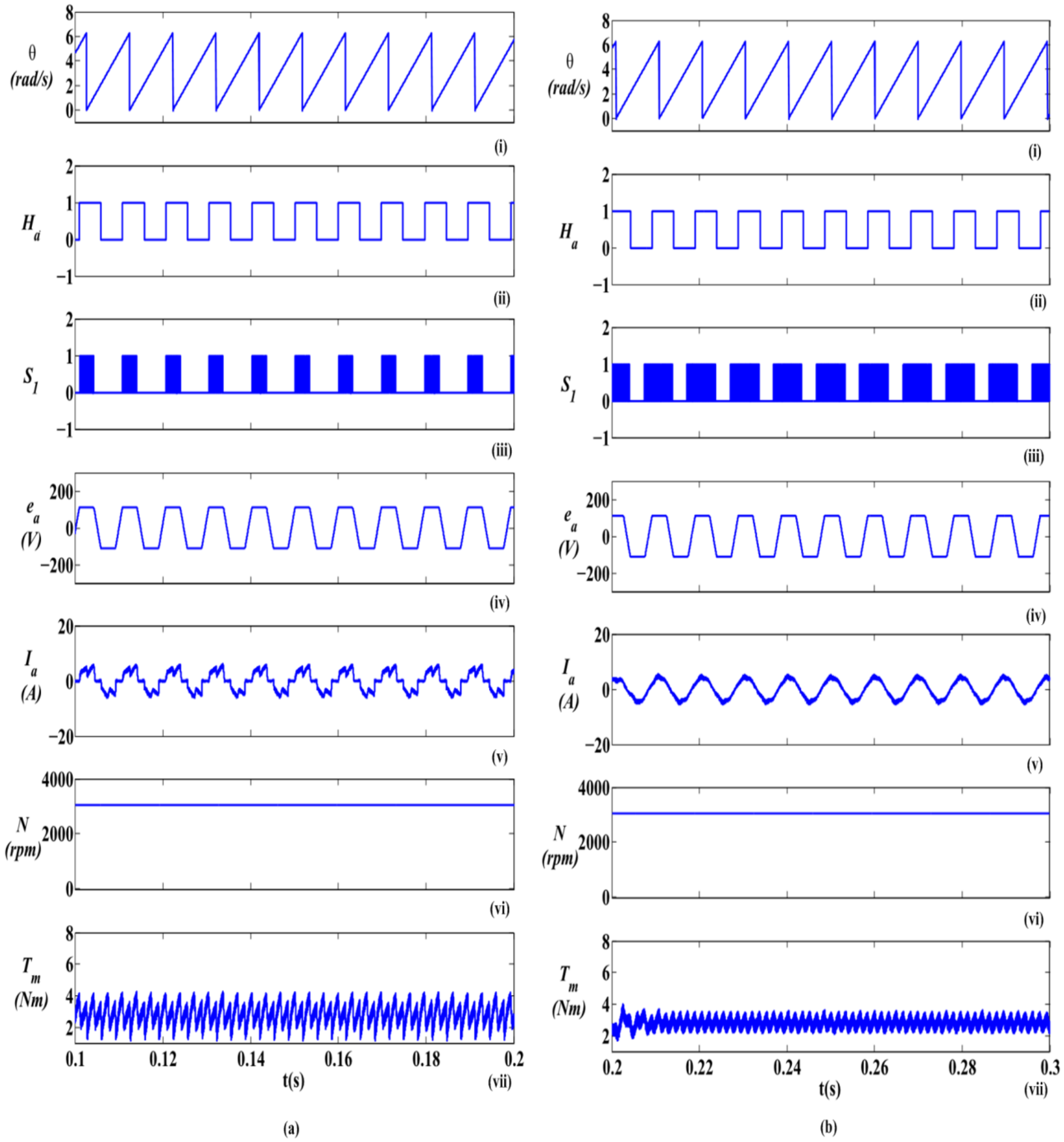

Fig. 5.4 Performance comparison of BLDC motor with (a) Conventional SSC & (b) MSPWM technique at a speed of 3000 rpm with applied load of 2.5

With the same speed of 3000 rpm and applied load changed to 5Nm as shown in Fig. 5.5(a) and (b) is to observe the performance of load change on the motor current, torque and DC bus utilization. The results demonstrates improved DC bus utilization with reduced torque ripple with the proposed MSPWM technique to prove its effectiveness with the sinusoidal currents in phase with the trapezoidal back emf. Figure 5.6 (a) and (b) gives the motor performance at a speed of 1750 rpm with a load of 5 Nm and 2.5 Nm. It can be observed that, with quasi square wave currents, the torque waveforms with conventional six-step control have sharp notches in the commutation region as compared to the MSPWM technique which provides a smooth torque curve with sinusoidal currents. At a speed of 1750rpm, some steady-state error in speed is observed with conventional SSC.

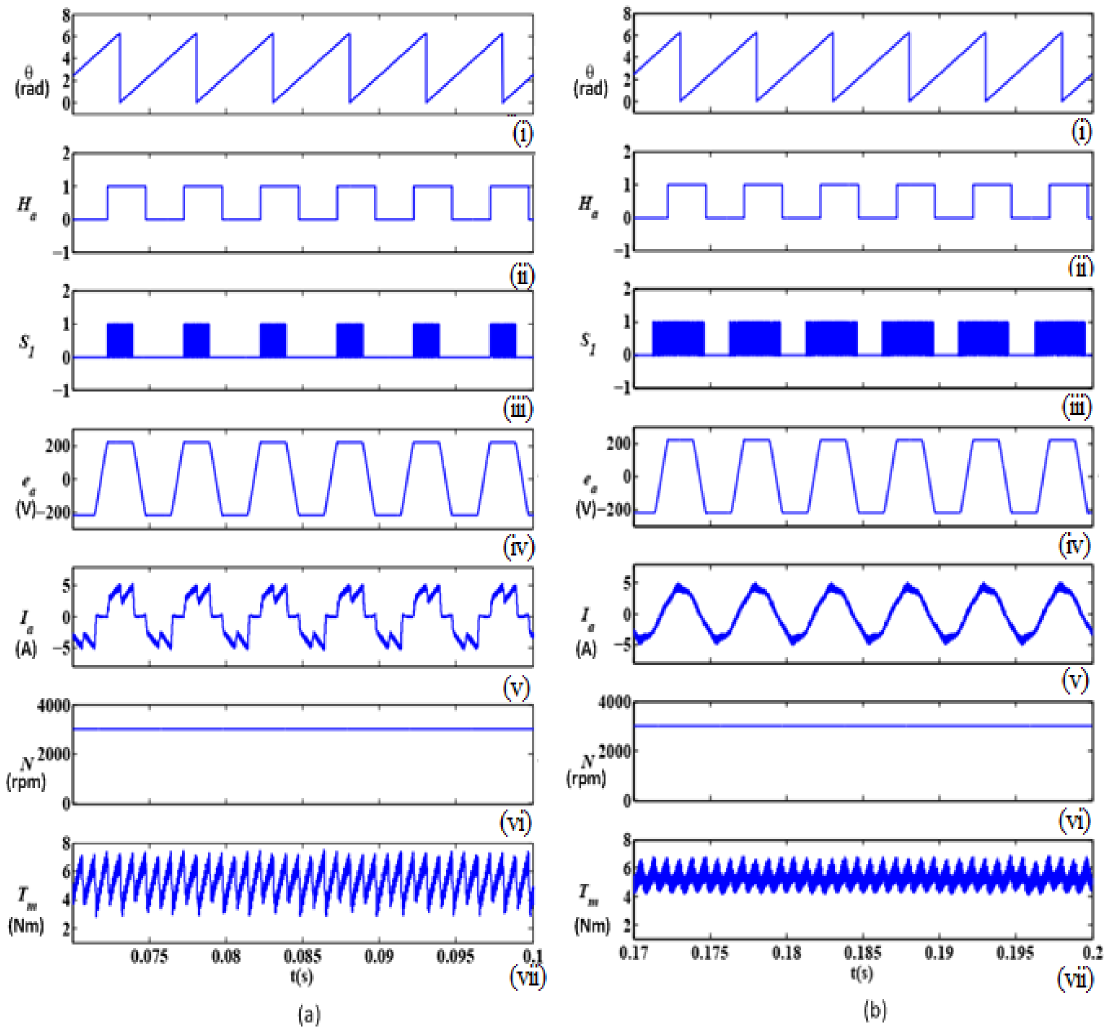

Fig. 5.5 Performance comparison of BLDC motor with (a) Conventional SSC (b) MSPWM technique at a speed of 3000 rpm with an applied load of 5Nm

It can be noticed that if speed is made constant and load is reduced by half, the motor current is reduced proportionately. In Fig.5.7(a) and (b), the motor speed is increased to 3000 rpm with the same applied load.As speed is increased there is an increase in stator voltage and the modulating voltage. The torque ripple seems to be reduced at a higher speed. Similarly, a comparison is shown of the MSPWM technique with SSC at a speed of 3000 rpm with an applied load of 2.5 Nm and 5 Nm is as in Fig. 5.8(a)and(b) respectively

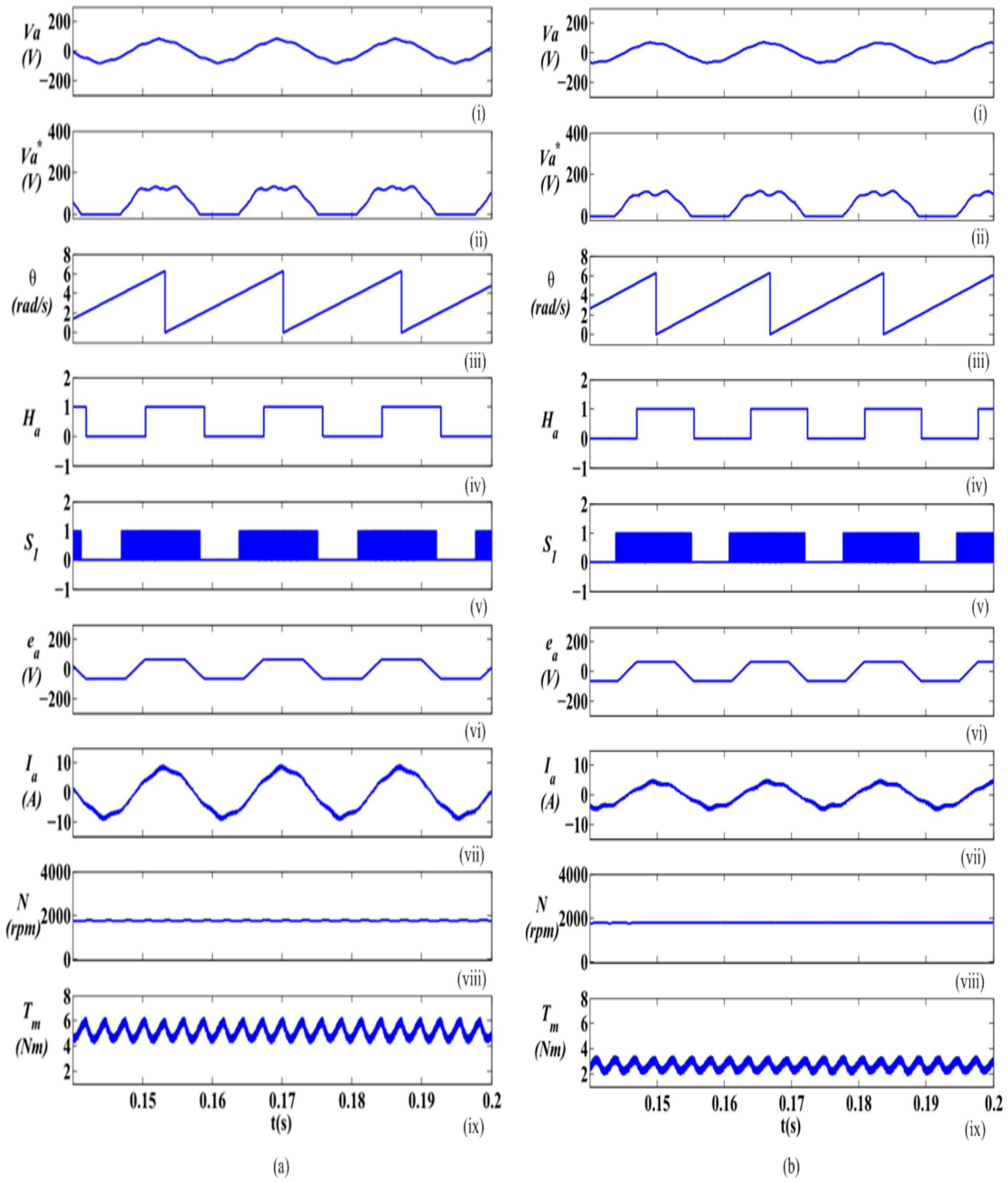

Fig. 5.6 Performance comparison of BLDC motor with MSPWM technique at a speed of 1750 rpm with applied load of (a) 5 Nm (b) 2.5 Nm

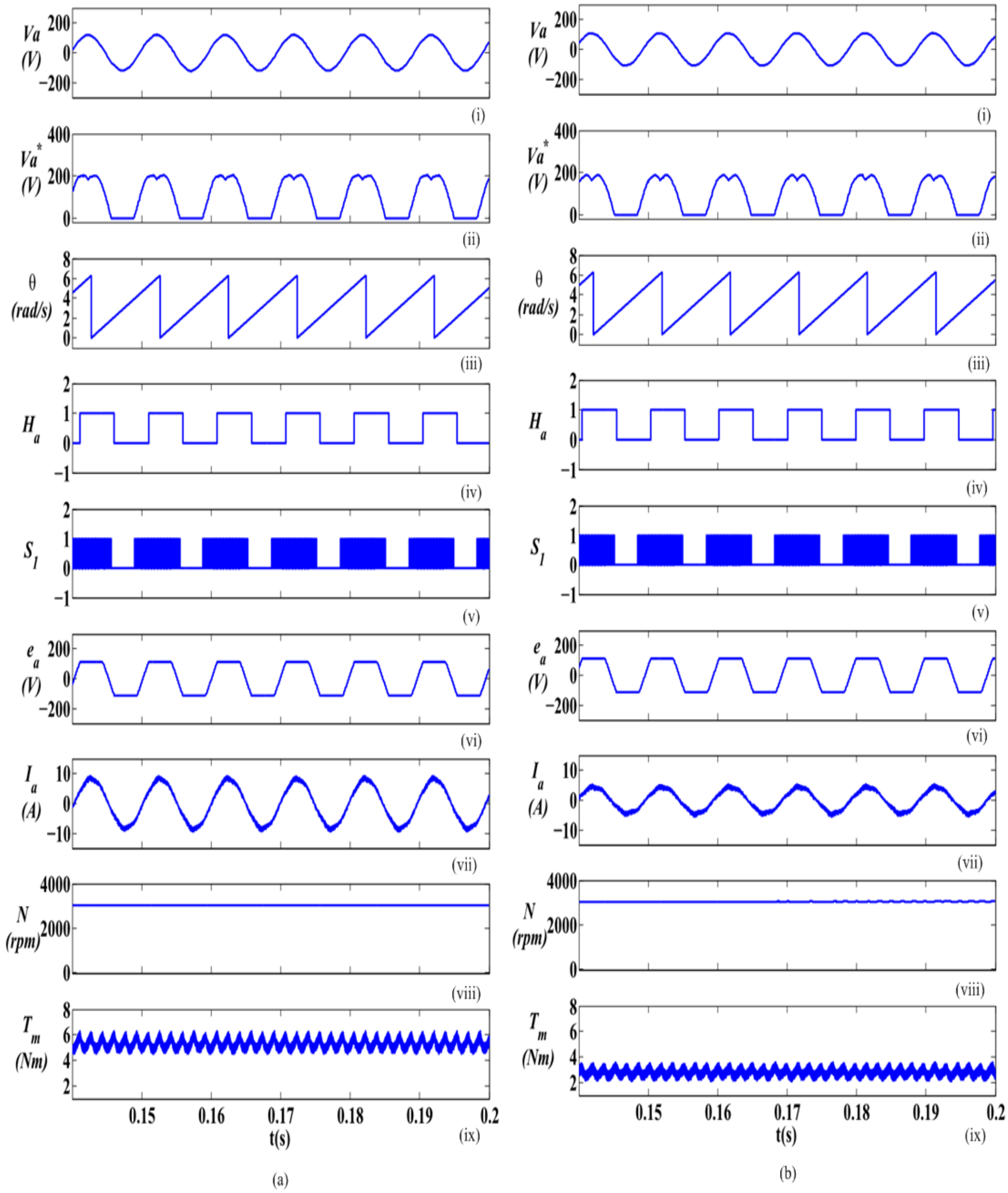

Fig. 5.7 Performance comparison of BLDC motor with MSPWM technique at a speed of 3000 rpm with applied load of (a) 5 Nm (b) 2.5 Nm

A similar comparison is also provided at a speed of 2500 rpm and 1750 rpm in Fig. 5.9(a) and (b) and Fig. 5.10(a) and (b) respectively which proves reduced torque ripple with the proposed MSPWM technique with sinusoidal stator current at different speeds and load condition as compared to the conventional SSC technique with the quasi square wave currents. Perfect tuning of the PI controller leads the motor to operate at the set speed which provides effective closed loop speed control.

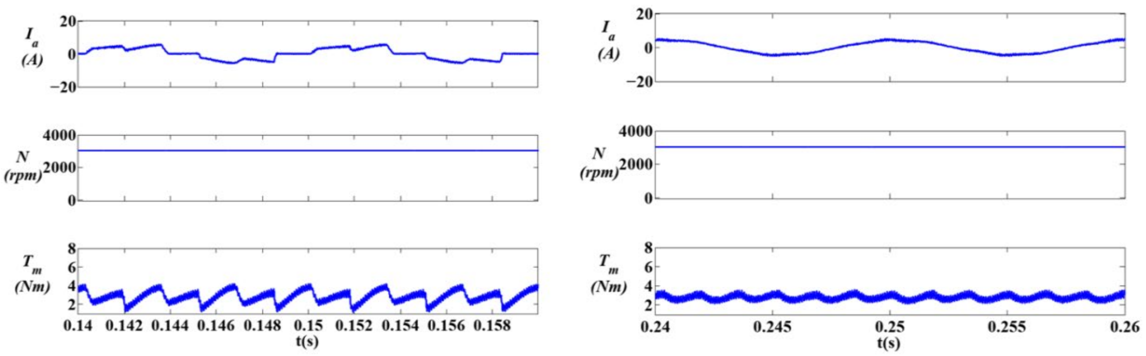

(a)

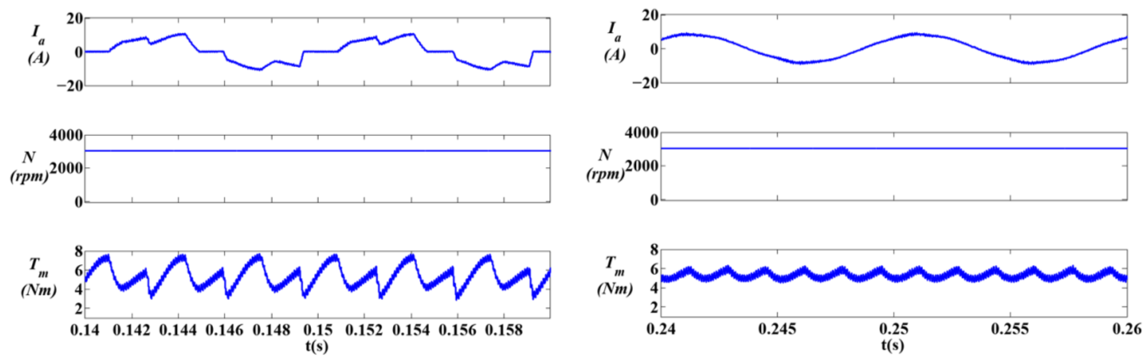

(b)

Fig. 5.8 Comparison of current, speed, and torque at a speed of 3000rpm with (a) Load of 2.5 Nm (b) Load of 5 Nm between the conventional SSC and the proposed MSPWM technique

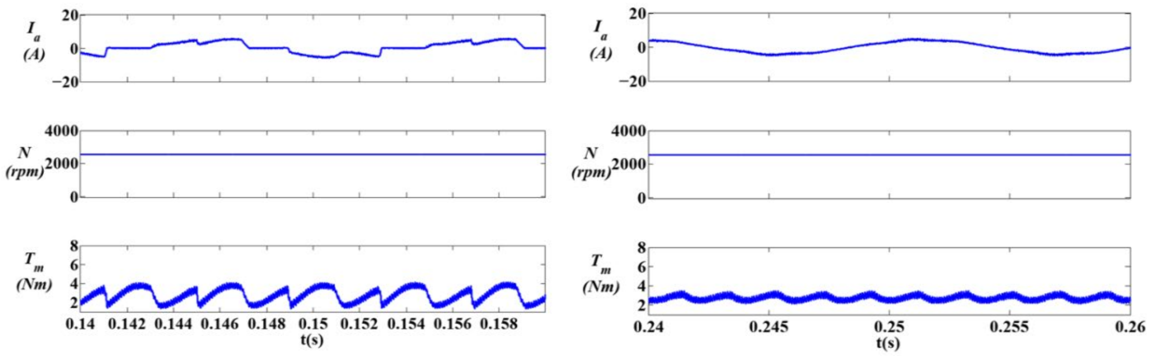

(a)

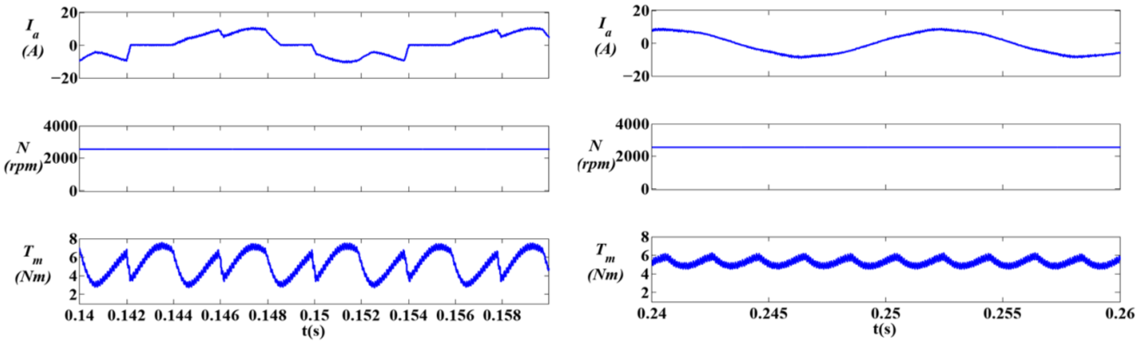

(b)

Fig. 5.9 Comparison of current, speed, and torque at a speed of 2500rpm with (a) Load of 2.5 Nm (b) Load of 5 Nm between the conventional SSC and the proposed MSPWM technique

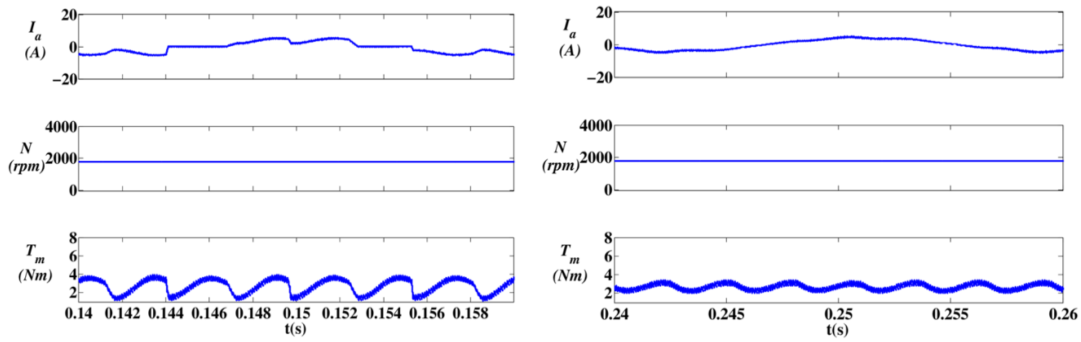

(a)

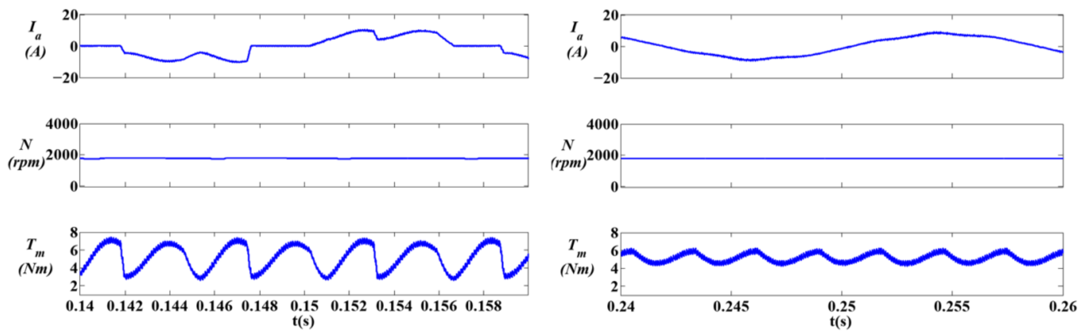

(b)

Fig. 5.10 Comparison of current, speed, and torque motor at a speed of 1750rpm with (a) Load of 2.5 Nm (b) Load of 5 Nm between the conventional SSC and the proposed MSPWM technique

5.5 Experimental results and discussion

To verify the MSPWM technique simulation results experiment is performed on different speeds above and below the rated speed. A voltage control loop is used to experiment using the MSPWM technique to control the speed of the motor with different load conditions. The overall system requirement for hardware implementation is as shown in Fig.3.15. The schematic block diagram of the overall system for the hardware implementation is as shown in Fig. 5.11

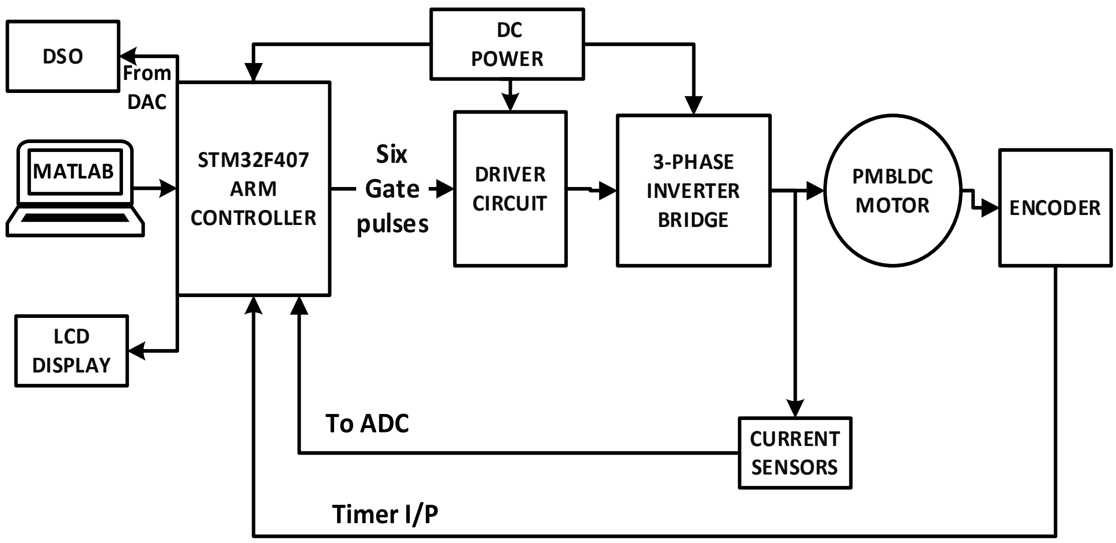

Fig. 5.11 Schematic block diagram of the overall system

The prototype consists of a 36 volt, 4 pole BLDC motor with a loading arrangement, STM32F407VG ARM controller discovery card with a clock frequency of 168 MHz, a three-phase voltage source inverter (VSI) with six insulated gate bipolar transistors (IGBTs), motor current sensor card, an intelligent IGBT driver card is provided to quarantine the low voltage controller circuit and high voltage power circuit, DC power circuit for the controller, driver card and inverter circuit. The rating of the motor is as given in Appendix. To generate the six gate pulses for six inverter switches, advanced Timer-8 is utilized. To prevent the shoot-through fault a dead band of 1 microsecond is provided. The value of switching frequency is 10 kHz, the sampling frequency of inner loop quantities is 25 kHz and the outer speed loop operates at 2.5 kHz. The set speed and actual speed are displayed on the LCD. The hardware results are captured using 4channel Digital Signal Oscilloscope.

The speed control loop is incorporated using a PI controller to process the error signal generated from the comparison between the reference speed and calculated speed. The 1250 ppr inbuilt shaft encoder used to calculate speed is given to the A9 and E9 pin to timer 1 of the controller card. A shift in speed from 1500rpm to 1000rpm and then from 1000rpm to 1500rpm is applied to witness the motor behaviour at constant load and with applied load change. The accurate tuning of the PI controller has led the drive to follow reference speed. A belt and pulley arrangement is provided for loading the motor. The loading is provided by increasing the tension on the belt. A maximum loading of 2.5 amperes can be provided for the given motor.

The experimental results provide the actual behavior of the presented technique in real-time on the BLDC motor drive operation. The conduction period of PWM pulses shows variation with the applied speed change and the response of the stator current and torque to the change in load. From Fig.5.12 and Fig.5.13, it can be discovered that using the MSPWM technique a discontinuous type saddled shape modulating signal is generated. The width of modulating reference signal is also increased with the speed. The conduction time is increased for a commanded speed of 1500 rpm.

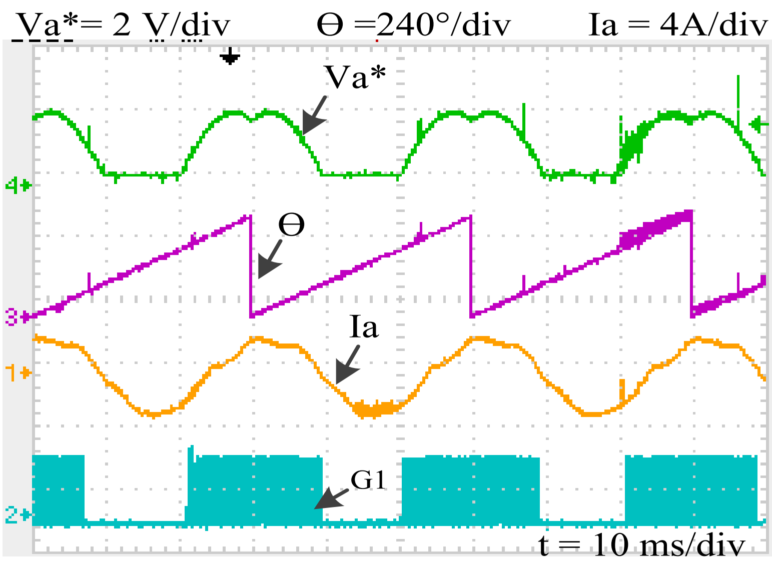

Fig. 5.12 Experimental waveforms of modulating voltage, theta, phase current, gate pulses for switch S1 at a speed of 1000 rpm under full load condition

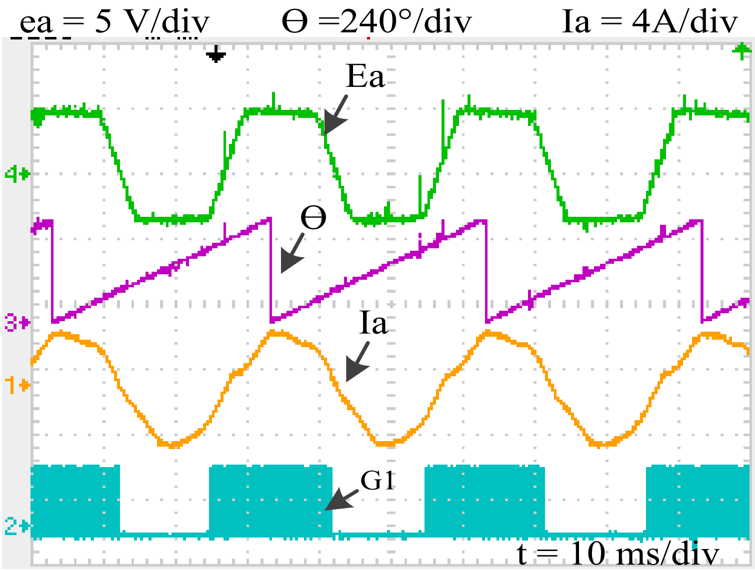

Fig. 5.13 Experimental waveforms of back emf, theta, phase current, gate pulses for switch S1 with MSPWM technique at a speed of 1000 rpm under full load condition

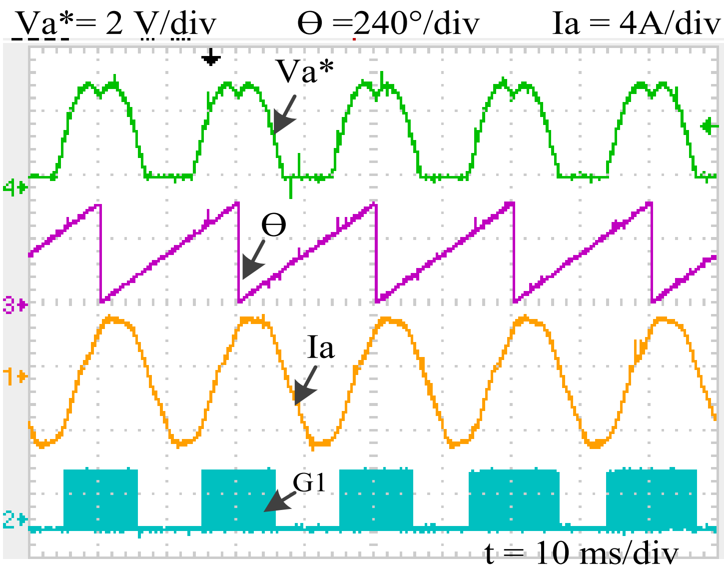

Fig. 5.14 Experimental waveforms of modulating voltage, theta, phase current, gate pulses for switch S1 at a speed of 1500rpm under full load condition

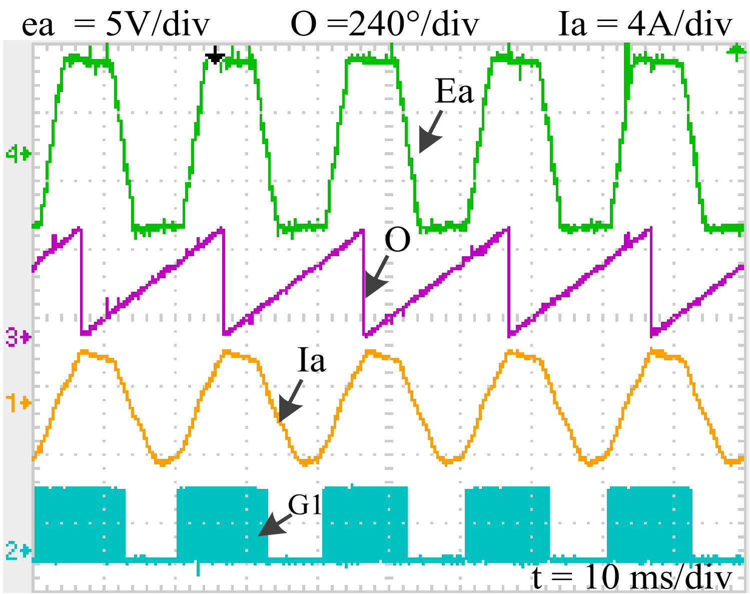

Fig. 5.15 Experimental waveforms of back emf, theta, phase current, gate pulses for switch S1 with MSPWM technique at a speed of 1500rpm under full load condition

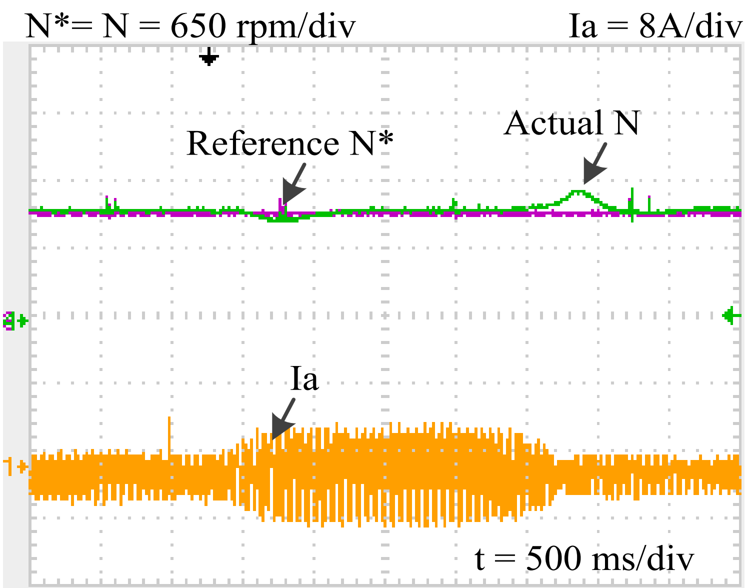

Fig. 5.16 Experimental waveforms of (a) comparison between actual speed and set speed, stator phase current with applied load change at a speed of 1000rpm

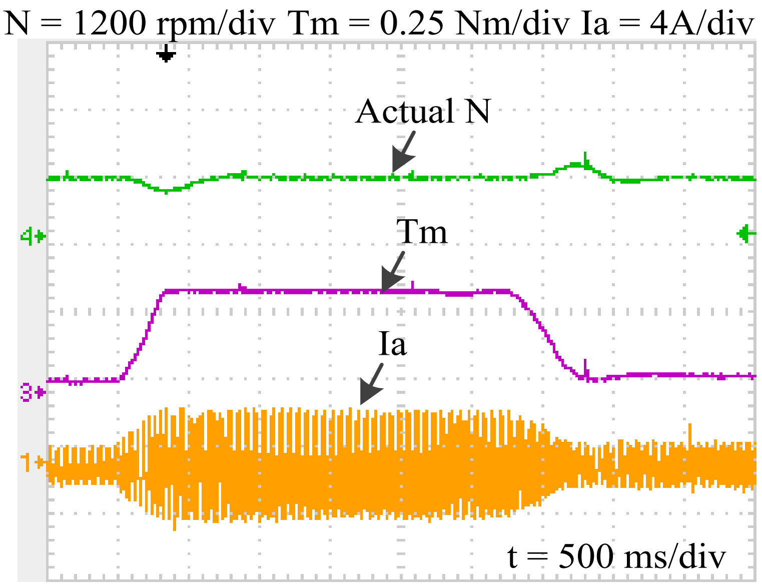

Fig. 5.17 Experimental waveforms of the behavior of actual motor speed, motor torque, and stator phase current with applied load change at a speed of 1000rpm

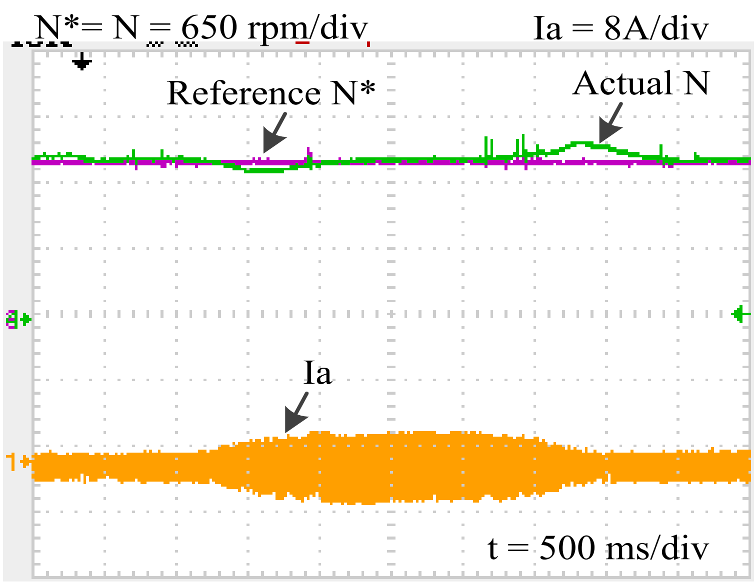

Fig. 5.18 Experimental waveforms of comparison between actual speed and set speed,stator phase current with applied load change at a speed of 1500rpm

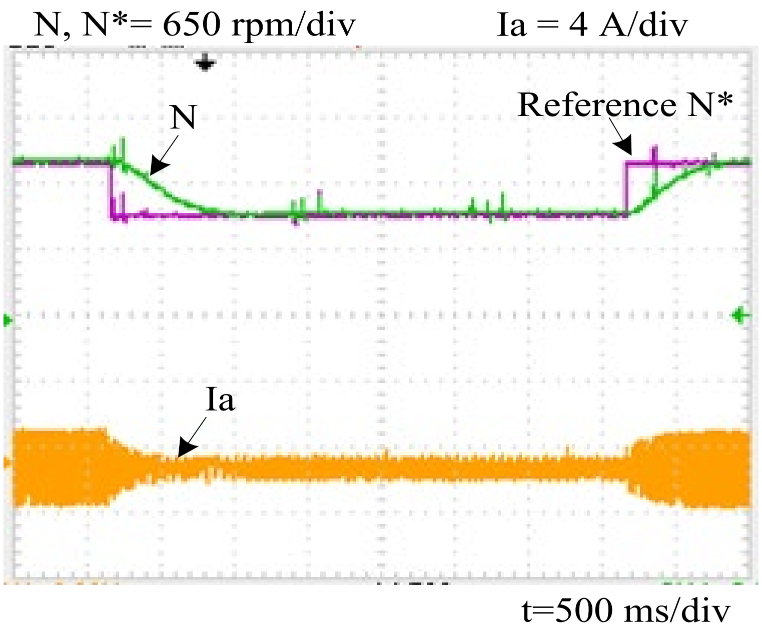

Fig. 5.19 Experimental waveforms of the behavior of stator phase current and actual motor speed with change in set speed from 1500rpm to 1000rpm under constant load condition

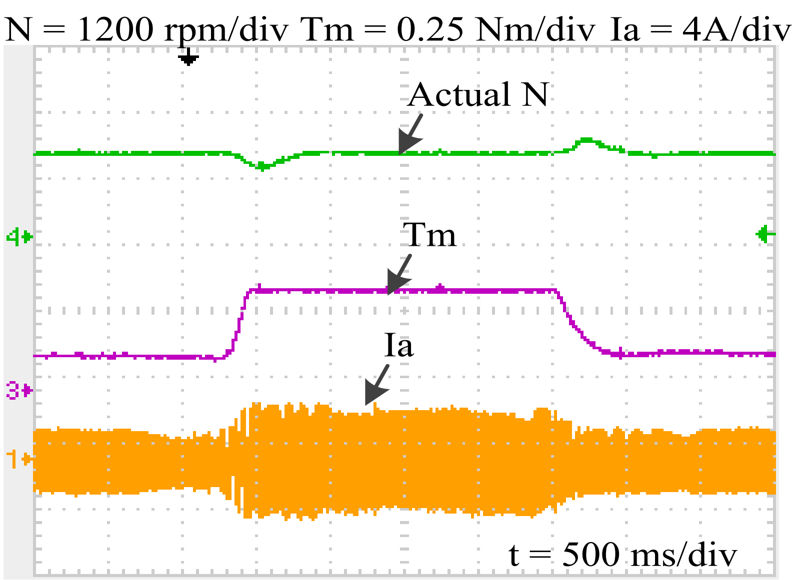

Fig. 5.20 Experimental waveforms of the behavior of actual motor speed, motor torque, and stator phase current with applied load change at a speed of 1500rpm

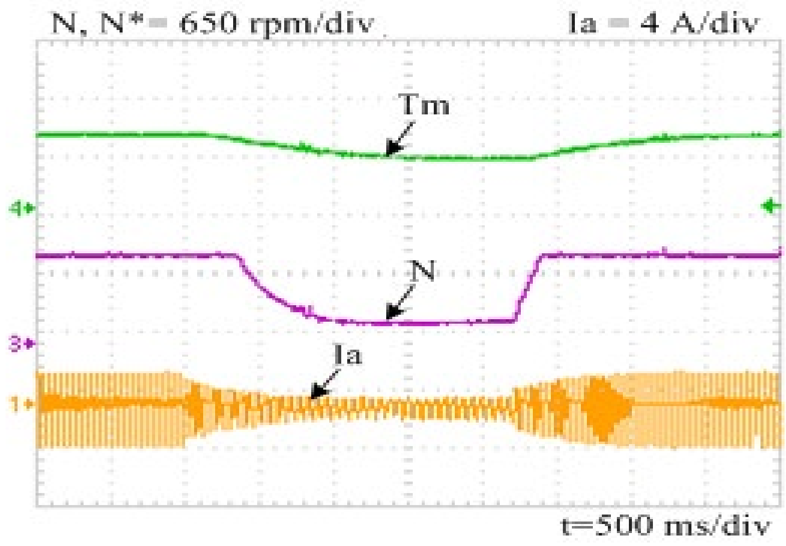

Fig. 5.21 Experimental waveforms of the behavior of actual motor torque, motor speed, and stator phase current with applied speed change from 1500rpm to 1000rpm under constant load condition

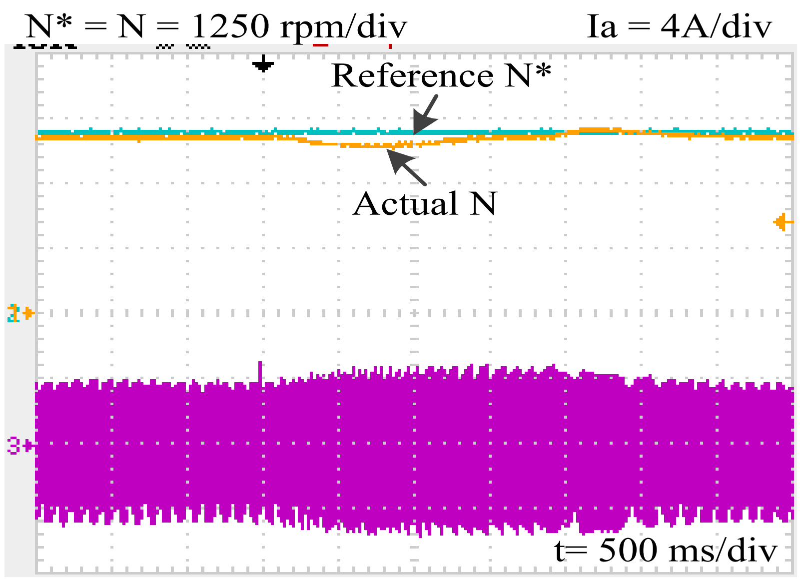

Fig. 5.22 Experimental waveforms of comparison between actual speed and set speed, stator phase current with applied load change at a speed of 3500rpm

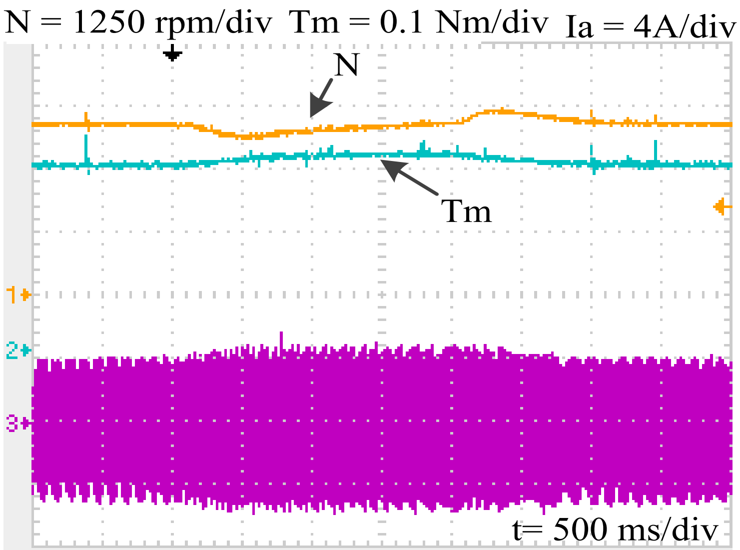

Fig. 5.23 Experimental waveforms of actual motor speed, motor torque, and stator phase current with applied load change at a speed of 3500rpm

The experimental results prove that using the presented MSPWM technique, sinusoidal stator currents are generated for a non-sinusoidal BLDC motor which helps in torque ripple reduction. As back emf being a function of rotor position and speed, it can be noted from Fig. 5.14 and Fig.5.15, that the magnitude of back emf increases with an increase in speed. With applied load changes the actual speed strictly follows the reference speed in Fig.5.16, Fig.5.18, and Fig.5.19 The stator currents react according to the applied load. Fig.5.17, Fig.5.20, and 5.23 show the variation in load on the motor torque with the speed remaining constant. Small dips can be spotted in the speed curve with sudden load change when the motor operates at a low speed about less than half the rated speed in Fig.5.17 and Fig.5.20. The dynamic response of the BLDC motor operation with applied speed change from 1500rpm to 100 rpm and its effect on motor phase current is as shown in Fig. 5.19. The actual motor speed takes around 500ms to achieve the set speed. As speed is decreased, the motor current also reduces. The variation in stator phase current can be observed with applied speed change from 1500rpm to 1000rpm under constant load conditions in Fig. 5.21. The variation in motor current and torque at a high speed of 3500rpm with applied load change can be observed in Fig.5.22 and Fig. 5.23 respectively. The PI controller takes about 300ms to regain the set speed for speed below half the rated speed but takes a longer time to respond to the load disturbance and reach the set speed when the motor is operated at a high speed of

3500rpm. The torque and speed waveforms are smooth with respect to the applied load changes. The stator current changes in accordance with the motor torque to meet the load demand.

This technique requires a high-speed processor as well as shaft encoder for instantaneous rotor position detection which makes the overall drive costly as compared to the conventional six-step operation. Since the proposed method controls motor operation in 3-phase conduction throughout the operation it may affect motor drive efficiency.

5.6 Comparative analysis of MSPWM technique with Six-Step Control

A comparative analysis between the proposed MSPWM technique and SSC showing torque ripple attenuation at different speed and loading conditions is provided in Table 5.2 and Table 5.3.

Table 5.2 Torque ripple with MSPWM technique

Speed (rpm)	1750		2500		3000	
Load Torque (Nm)	5	2.5	5	2.5	5	2.5
Torque ripple (Nm)	2.5	1.6	2	1.3	1.8	1.2
Ripple factor	0.5	0.64	0.4	0.52	0.36	0.48

Table 5.3 Torque ripple with conventional SSC technique

Speed (rpm)	1750		2500		3000	
Load Torque (Nm)	5	2.5	5	2.5	5	2.5
Torque ripple (Nm)	5.3	2.8	5	2.6	4.8	2.5
Ripple factor	1.06	1.12	1	1.04	0.96	1

Fig. 5.22 provides the graphical comparison of torque ripple under different speed and loading conditions for the six-step control and the proposed MSPWM technique. It shows that the commutation torque ripple is reduced by 50% with the MSPWM technique at all

speeds with the loading of 2.5Nm with 3-ΦO as compared to the conventional six-step control with 2-ΦO. With an applied load of 5 Nm, it can be observed that the torque ripple is reduced by more than 50% with the proposed MSPWM technique as compared to the six-step control at all set speeds. From the plot, it can be concluded that the proposed MSPWM technique with 3-ΦO gives better performance.

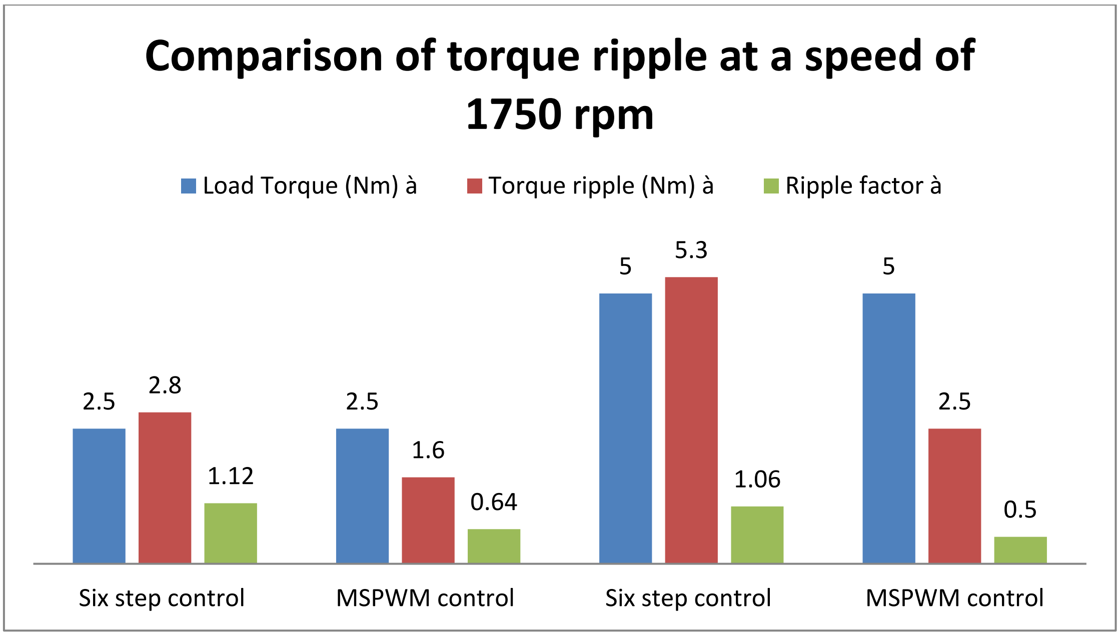

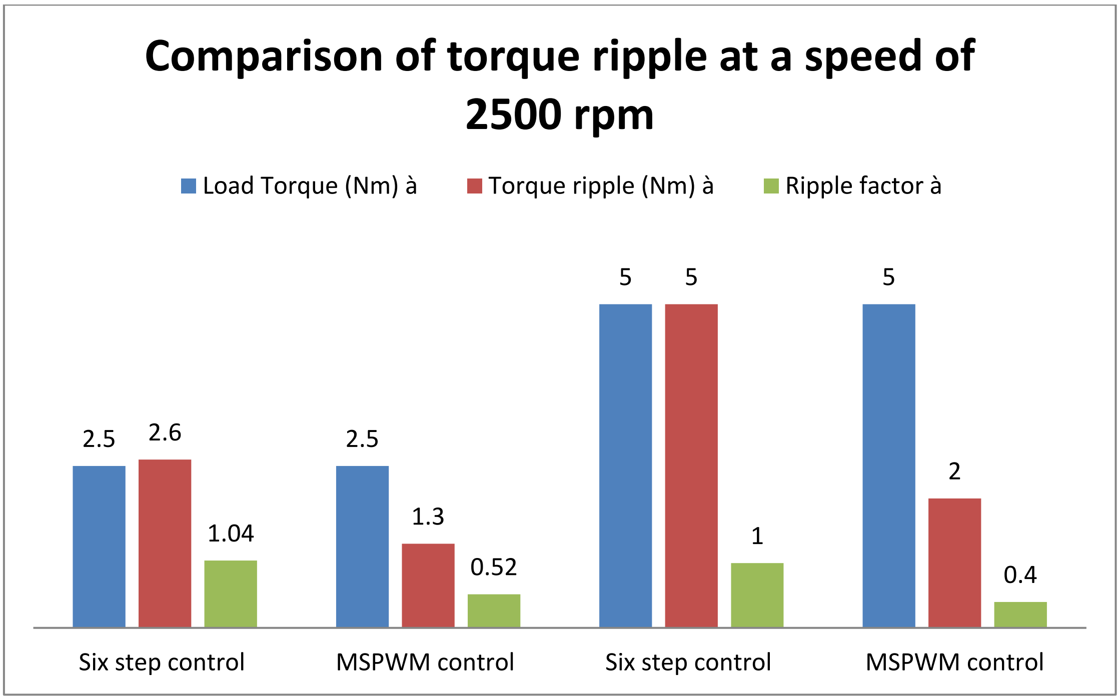

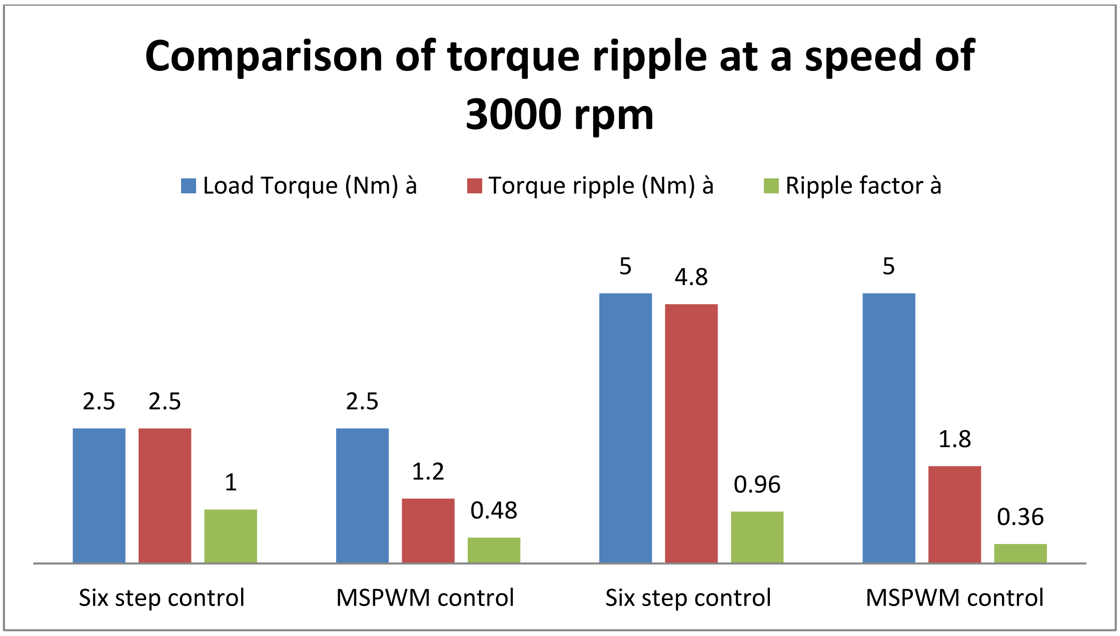

Fig. 5.24 Comparative analysis between the proposed MSPWM technique and six-step control showing torque ripple attenuation at different speed and loading condition

5.7 Comparison of proposed techniques with the existing 2-ΦO, 2-3ΦO and 3-ΦO

A comparison of the proposed technique with known techniques for the BLDC motor based on various parameters under 2-ΦO, 2-3ΦO and 3-ΦO is shown in Table 5.4.

The comparison among the various control techniques depicts that the BLDC motor performance is deteriorated with no complex control required when it is operated in two phase conduction mode. The motor performance is improved with a combined two phase and three phase conduction mode with medium control complexity as αβ coordinate transformation is required. The proposed MTSDTC with ONPWM and PWMON provides reduced switching losses increasing the overall efficiency of the drive. The ONPWM also provides reduced torque ripple resulting in smooth operation of the drive. The three phase conduction needs phase transformation in dq plane increasing the control complexity. The BLDC motor with sinusoidal current in phase with the trapezoidal back emf results in reduced stator copper losses. The sinusoidal stator currents provides reduced torque with smooth operation but requires shaft encoder for continuous rotor position or a rotor position that increases the overall cost of the drive. The proposed MSPWM technique is much simple with only one PI controller as compared to the SVM technique.

Table 5.4 Comparison of proposed techniques with the existing techniques

Techniques →	2-ΦO SSC	2-ΦO Hysteresis	2-3ΦO TSDTC	Proposed 2-3ΦO MTSDTC ONPWM	Proposed 2-3ΦO MTSDTC ONPWM	3-ΦO SVM	Proposed 3-ΦO MSPWM
Nature of Back emf and Current	Trapezoidal emf & Quasi square current	Trapezoidal emf & Quasi square current	Trapezoidal emf & Quasi square current	Trapezoidal emf & Quasi square current	Trapezoidal emf & Quasi square current	Trapezoidal emf & sinusoidal current	Trapezoidal emf & sinusoidal current
Phase Conduction	Two	Two	Two & Three	Two & Three	Two & Three	Three	Three
Coordinate transformation	No	No	abc to αβ	abc to αβ	abc to αβ	abc to dq	abc to dq
Control tuning	PI gain	Hysteresis band	Hysteresis band	Hysteresis band	Hysteresis band	PI gain	PI gain
PWM modulator	No	No	No	No	No	Yes	Yes
Current control	No	Yes	No	No	No	Yes	No
Switching frequency	Constant	Variable, depending on the operating point	Variable, depending on the operating point	Variable, depending on the operating point	Variable, depending on the operating point	Constant	Constant
Continuous Requirement of rotor position	No	No	No	No	No	Yes	Yes
Torque ripple	High	High	Medium	**Low**	**High**	Low	**Low**
Complexity of Control	Less	Less	Medium	Medium	Medium	High	**Low**
Processing time	High	High	**Low**	**Low**	**Low**	High	**Low**
Dynamic torque response	low	low	High	High	High	low	**medium**
Switching Losses	Low	Low	High	**Low**	**Low**	High	High
Stator Cu loss	High	Medium	High	High	High	Low	**Low**
Overall efficiency	Low	Low	Medium	**High**	**High**	High	**High**
Motor Performance	Low	Low	Medium	**High**	**High**	High	**High**
Cost	Low	Low	Low	**Low**	**Low**	High	High

5.8 Conclusion

A simple closed-loop control technique of BLDC motor and torque ripple attenuation using sinusoidal excitation of the phase winding with trapezoid back emf is accorded here with 3-ΦO. The detailed analysis of Modified Sinusoidal Pulse Width Modulation(MSPWM) technique for closed-loop speed control of BLDC motor is discussed and simulation is performed to verify the performance of BLDC motor drive at different speed and load. The results are compared with the widely used six-step control of the BLDC motor. A better dynamic response is achieved and torque ripple is effectively reduced by the proposed method. The utilization of the DC link is also improved compared to conventional six-step control. The motor dynamic response is improved using only one PI controller as compared to the FOC and DTC techniques which reduces the control complexity. The proposed method is experimentally validated and dynamic performance of the drive with closed-loop speed control at wide range of speed and load is verified.